GEOPHYSICS, VOL. 64, NO. 4 (JULY-AUGUST 1999); P. 1219–1229, 7 FIGS., 1 TABLE.

Moveout inversion of *P*-wave data for horizontal transverse isotropy

Pedro Contreras*, Vladimir Grechka‡, and Ilya Tsvankin‡

ABSTRACT

The transversely isotropic model with a horizontal symmetry axis (HTI media) has been extensively used in seismological studies of fractured reservoirs. In this paper, a parameter-estimation technique originally developed by Grechka and Tsvankin for the more general orthorhombic media is applied to horizontal transverse isotropy. Our methodology is based on the inversion of azimuthally-dependent *P*-wave normal-moveout (NMO) velocities from horizontal and dipping reflectors.

If the NMO velocity of a given reflection event is plotted in each azimuthal direction, it forms an ellipse determined by three combinations of medium parameters. The NMO ellipse from a horizontal reflector in HTI media can be inverted for the azimuth β of the symmetry axis, the vertical velocity V_{P0}, and the Thomsen-type anisotropic parameter $\delta^{(V)}$. We describe a technique for obtaining the remaining (for *P*-waves) anisotropic parameter $\eta^{(V)}$ (or $\epsilon^{(V)}$) from the NMO ellipse corresponding to a dipping reflector of arbitrary azimuth. The interval parameters of vertically inhomogeneous HTI media are recovered using the generalized Dix equation that operates with NMO ellipses for horizontal and dipping events. High accuracy of our method is confirmed by inverting a synthetic multiazimuth *P*-wave data set generated by ray tracing for a layered HTI medium with depth-varying orientation of the symmetry axis.

Although estimation of $\eta^{(V)}$ can be carried out by the algorithm developed for orthorhombic media, for more stable results the HTI model has to be used from the outset of the inversion procedure. It should be emphasized that *P*-wave conventional-spread moveout data provide enough information to distinguish between HTI and lower-symmetry models. We show that if the medium has the orthorhombic symmetry and is sufficiently different from HTI, the best-fit HTI model cannot match the NMO ellipses for both a horizontal and a dipping event.

The anisotropic coefficients responsible for *P*-wave moveout can be combined to estimate the crack density and predict whether the cracks are fluid-filled or dry. A unique feature of the HTI model that distinguishes it from both vertical transverse isotropy and orthorhombic media is that moveout inversion provides not just zero-dip NMO velocities and anisotropic coefficients, but also the true vertical velocity. As a result, reflection *P*-wave data acquired over HTI formations can be used to build velocity models in depth and perform anisotropic depth processing.

INTRODUCTION

Horizontal transverse isotropy (HTI) (Figure 1) is a common model in shear-wave studies of fractured reservoirs that describes a system of parallel vertical penny-shaped cracks embedded in an isotropic host rock (e.g., Thomsen, 1988). The fractional difference between the velocities of split *S*-waves at vertical incidence is proportional to the crack density (Thomsen, 1995) and, therefore, provides important insight into the properties of the fractured reservoir. An alternative approach to parameter estimation in HTI media is based on the inversion of azimuthally-dependent reflection traveltimes.

Tsvankin (1997a) gave an exact equation for normal-moveout (NMO) velocity (analytically defined in the zero-spread limit) of pure modes in a horizontal HTI layer and showed that it represents an ellipse with the axes parallel to the vertical symmetry planes of the medium. For *P*-waves, the NMO ellipse depends on the azimuth of the symmetry axis β, the vertical velocity V_{P0}, and the anisotropic coefficient $\delta^{(V)}$ analogous to the parameter δ introduced by Thomsen (1986) for transversely isotropic (TI) models with a vertical symmetry axis (VTI media). The superscript "(V)" in $\delta^{(V)}$ stands for the "equivalent" VTI medium and is used to avoid confusion with the generic Thomsen coefficients defined with

Manuscript received by the Editor February 2, 1998; revised manuscript received November 18, 1998.
*Intevep-PDVSA, P.O. Box 76343, Caracas 1070A DF, Venezuela. E-mail: pecontrer@intevep.pdv.com.
‡Colorado School of Mines, Center for Wave Phenomena, Department of Geophysics, Golden, Colorado 80401. E-mail: vgrechka@dix.mines.edu; ilya@dix.mines.edu.

respect to the symmetry axis (Rüger, 1997; Tsvankin, 1997a). P-wave kinematic signatures in HTI media are controlled not just by β, V_{P0}, and $\delta^{(V)}$, but also by another anisotropic coefficient, $\epsilon^{(V)}$, that is close to the fractional difference between the symmetry-direction P-wave velocity and V_{P0}. Tsvankin (1997a) suggested obtaining $\epsilon^{(V)}$ either by combining NMO velocities of the P-wave and slow S-wave (the wave polarized perpendicular to the cracks at vertical incidence) or by inverting dip-dependent P-wave moveout in the vertical plane that contains the symmetry axis (the "symmetry-axis plane"). The inversion of dip moveout in the symmetry-axis plane is based on a 2-D NMO equation (Tsvankin, 1995) and, therefore, can be applied only if the symmetry axis lies in the dip plane of the reflector. In principle, the parameter $\epsilon^{(V)}$ can also be recovered from nonhyperbolic (long-spread) moveout, as described by Al-Dajani and Tsvankin (1998). The set of the three P-wave moveout coefficients (V_{P0}, $\delta^{(V)}$, $\epsilon^{(V)}$) can be used to reconstruct P-wave phase velocity and perform seismic imaging, as well as to estimate the crack density and investigate the contents of the fracture network (Rüger and Tsvankin, 1997; Tsvankin, 1997a).

In this paper, we present an algorithm designed to obtain the parameter $\epsilon^{(V)}$ and, if necessary, the symmetry-axis direction using the azimuthally-dependent NMO velocity from a dipping reflector with arbitrary orientation. As shown by Grechka and Tsvankin (1998), the azimuthal variation of pure-mode NMO velocity typically is described by an ellipse for any inhomogeneous arbitrary anisotropic medium. Since the ellipse is fully determined by three quantities (e.g., by its orientation and semiaxes), only three combinations of medium parameters can be found from multiazimuth NMO-velocity measurements of a certain mode. Clearly, these parameter combinations depend on the anisotropy of the model for which the inversion is carried out. For example, Grechka and Tsvankin (1998) proved that the P-wave NMO ellipse for dipping events in VTI media, expressed through the horizontal slowness components of the zero-offset ray, is a function of two Alkhalifah-Tsvankin (1995) parameters: the "zero-dip" NMO velocity from a horizontal reflector $V_{\rm nmo}(0)$ and the "anellipticity" coefficient η. For the more complicated azimuthally-anisotropic model with orthorhombic symmetry, NMO velocity of P-waves depends on six quantities: the azimuth of one of the vertical symmetry planes, the zero-dip NMO velocities in the symmetry-plane directions $V_{\rm nmo}^{(1,2)}$, and three anisotropic coefficients $\eta^{(1,2,3)}$ defined similarly to the parameter η for VTI media. Grechka and Tsvankin (1999), who obtained this result, also developed a parameter-estimation procedure to find the symmetry-plane orientation and five moveout parameters from the NMO ellipses of a horizontal and a dipping event.

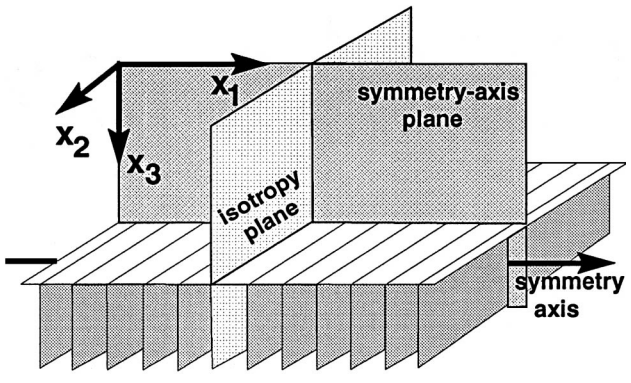

FIG. 1. HTI model is used to describe a system of parallel vertical cracks in an isotropic background medium (after Rüger, 1997). The two vertical symmetry planes are called the "isotropy plane" (parallel to the cracks) and the "symmetry-axis plane" (orthogonal to the cracks).

The method of Grechka and Tsvankin (1999) can be applied to the moveout inversion in HTI media because horizontal transverse isotropy can be considered as a special case of the more general orthorhombic model. The transition from orthorhombic to HTI media becomes particularly simple within the framework of Tsvankin's (1997b) notation for orthorhombic anisotropy. For instance, the P-wave NMO ellipse from a horizontal reflector in HTI media can be obtained from the corresponding NMO ellipse in orthorhombic media just by setting the appropriate δ coefficient to zero. Likewise, the P-wave NMO velocity of dipping events in HTI media depends on only one η coefficient ($\eta^{(V)}$) directly related to the parameter $\epsilon^{(V)}$. Since NMO ellipse is described by three independent quantities, there is a useful redundancy in estimating the parameter $\eta^{(V)}$. We discuss the moveout inversion for $\eta^{(V)}$ in HTI media and show that it is more stable than the inversion for the three coefficients $\eta^{(1,2,3)}$ in orthorhombic media.

Extention of the moveout-inversion algorithm to vertically-inhomogeneous HTI media is based on the generalized Dix equation of Tsvankin et al. (1997). This equation expresses the exact NMO velocity for a stack of layers above a dipping reflector as an average of the matrices responsible for the interval NMO ellipses. Dix-type differentiation makes it possible to find the interval values of β, V_{P0}, $\delta^{(V)}$, and $\epsilon^{(V)}$, which are sufficient to perform depth processing in HTI media. The performance of the algorithm is illustrated by numerical examples for a single HTI layer and a stratified HTI model with depth-varying azimuth of the symmetry axis.

NOTATION FOR HTI AND ORTHORHOMBIC MEDIA

Since our approach is based on the methodology of Grechka and Tsvankin (1999) developed for orthorhombic media, we need to review the relation between the parameters of orthorhombic and HTI models. An orthorhombic (or orthotropic) symmetry system may be caused, for instance, by a set of parallel vertical cracks embedded in a background VTI medium (Figure 2) or by two orthogonal (or identical nonorthogonal) vertical crack systems in a purely isotropic or VTI matrix (e.g., Wild and Crampin, 1991; Schoenberg and Helbig, 1997). Regardless of the reasons for orthorhombic anisotropy, it is characterized by three mutually orthogonal planes of mirror symmetry, which are conventionally chosen as the coordinate planes. Tsvankin (1997b) used an identical form of the Christoffel equation within the symmetry planes of orthorhombic and VTI media to parameterize orthorhombic models by two vertical velocities (the "isotropic" quantities) and seven VTI-style dimensionless anisotropic coefficients. This notation, based on the same principle as Thomsen (1986) parameters for vertical transverse isotropy, is particularly well-suited for traveltime inversion (Grechka and Tsvankin, 1999). The expressions for Tsvankin's parameters in terms of the stiffness coefficients c_{ij} and density ρ are given below:

1) V_{P0} is P-wave vertical velocity:

$$V_{P0} \equiv \sqrt{\frac{c_{33}}{\rho}}. \tag{1}$$

2) V_{S0} is the vertical velocity of the S-wave polarized in the x_1-direction:

$$V_{S0} \equiv \sqrt{\frac{c_{55}}{\rho}}. \tag{2}$$

3) $\epsilon^{(2)}$ is the VTI parameter ϵ in the $[x_1, x_3]$ symmetry plane normal to x_2-axis (this explains the superscript "2"):

$$\epsilon^{(2)} \equiv \frac{c_{11} - c_{33}}{2\,c_{33}}. \tag{3}$$

$\epsilon^{(2)}$ is close to the fractional difference between the P-wave velocities in the x_1- and x_3-directions.

4) $\delta^{(2)}$ is the VTI parameter δ in the $[x_1, x_3]$-plane:

$$\delta^{(2)} \equiv \frac{(c_{13} + c_{55})^2 - (c_{33} - c_{55})^2}{2c_{33}(c_{33} - c_{55})}. \tag{4}$$

Within the $[x_1, x_3]$-plane, $\delta^{(2)}$ is responsible for near-vertical P-wave velocity and influences the velocity of the in-plane polarized shear wave.

5) $\gamma^{(2)}$ is the VTI parameter γ in the $[x_1, x_3]$-plane:

$$\gamma^{(2)} \equiv \frac{c_{66} - c_{44}}{2c_{44}}. \tag{5}$$

$\gamma^{(2)}$ is close to the fractional difference between the SH-wave velocities in the x_1- and x_3-directions (by the SH-wave, we mean the shear wave that propagates in the $[x_1, x_3]$-plane being polarized in the x_2-direction).

6) $\epsilon^{(1)}$ is the VTI parameter ϵ in the $[x_2, x_3]$ symmetry plane:

$$\epsilon^{(1)} \equiv \frac{c_{22} - c_{33}}{2c_{33}}. \tag{6}$$

$\epsilon^{(1)}$ is close to the fractional difference between the P-wave velocities in the x_2- and x_3-directions.

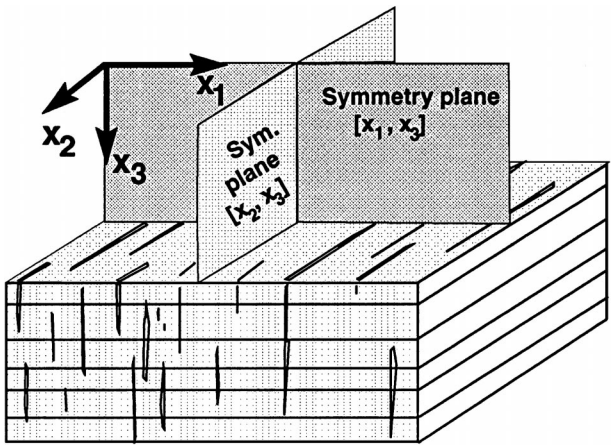

FIG. 2. Orthorhombic media have three mutually orthogonal planes of mirror symmetry. One of the reasons for orthorhombic anisotropy is a combination of parallel vertical cracks and vertical transverse isotropy in the background medium.

7) $\delta^{(1)}$ is the VTI parameter δ in the $[x_2, x_3]$-plane:

$$\delta^{(1)} \equiv \frac{(c_{23} + c_{44})^2 - (c_{33} - c_{44})^2}{2c_{33}(c_{33} - c_{44})}. \tag{7}$$

Within the $[x_2, x_3]$-plane, $\delta^{(1)}$ is responsible for near-vertical P-wave velocity and influences the velocity of the in-plane polarized shear wave.

8) $\gamma^{(1)}$ is the VTI parameter γ in the $[x_2, x_3]$-plane:

$$\gamma^{(1)} \equiv \frac{c_{66} - c_{55}}{2c_{55}}. \tag{8}$$

$\gamma^{(1)}$ is close to the fractional difference between the SH-wave velocities in the x_2-and x_3-directions (here, the SH-wave is polarized in the x_1-direction).

9) $\delta^{(3)}$ is the VTI parameter δ in the $[x_1, x_2]$-plane (x_1 plays the role of the symmetry axis):

$$\delta^{(3)} \equiv \frac{(c_{12} + c_{66})^2 - (c_{11} - c_{66})^2}{2c_{11}(c_{11} - c_{66})}. \tag{9}$$

An important parameter combination that we will use below is the shear-wave splitting coefficient at vertical incidence:

$$\gamma^{(S)} \equiv \frac{c_{44} - c_{55}}{2c_{55}} = \frac{\gamma^{(1)} - \gamma^{(2)}}{1 + 2\gamma^{(2)}}. \tag{10}$$

$\gamma^{(S)}$ is close to the fractional difference between the velocities of split S-waves at vertical incidence.

Only a subset of these parameters (V_{P0}, $\epsilon^{(1,2)}$, and $\delta^{(1,2,3)}$) controls P-wave kinematic signatures for orthorhombic media (Tsvankin, 1997b). Furthermore, Grechka and Tsvankin (1999) showed that P-wave normal-moveout velocity for horizontal and dipping reflectors, expressed through the horizontal slowness components of the zero-offset ray, depends on just five parameter combinations. These moveout parameters include the symmetry-plane NMO velocities from a horizontal reflector,

$$V_{\rm nmo}^{(i)} = V_{P0}\sqrt{1 + 2\delta^{(i)}}, \qquad (i = 1, 2) \tag{11}$$

and three anisotropic coefficients $\eta^{(1,2,3)}$ defined by analogy with the Alkhalifah-Tsvankin (1995) parameter η in VTI media.

$\eta^{(2)}$ is the VTI parameter η in the vertical symmetry plane $[x_1, x_3]$:

$$\eta^{(2)} \equiv \frac{\epsilon^{(2)} - \delta^{(2)}}{1 + 2\,\delta^{(2)}}; \tag{12}$$

$\eta^{(1)}$ is the VTI parameter η in the vertical symmetry plane $[x_2, x_3]$:

$$\eta^{(1)} \equiv \frac{\epsilon^{(1)} - \delta^{(1)}}{1 + 2\,\delta^{(1)}}; \tag{13}$$

$\eta^{(3)}$ is the VTI parameter η in the horizontal symmetry plane $[x_1, x_2]$ (x_1 plays the role of the symmetry axis):

$$\eta^{(3)} \equiv \frac{\epsilon^{(1)} - \epsilon^{(2)} - \delta^{(3)}\left(1 + 2\epsilon^{(2)}\right)}{\left(1 + 2\epsilon^{(2)}\right)\left(1 + 2\delta^{(3)}\right)}. \tag{14}$$

For the HTI model that may be considered as a special case of orthorhombic media, the number of independent parameters reduces from nine to five. If we align the symmetry axis with the x_1-direction (Figure 1), the velocities of all three modes in the $[x_2, x_3]$-plane (the isotropy plane) become constant, and the anisotropic coefficients in this plane [equations (6)–(8)] vanish (Tsvankin, 1997b):

$$\epsilon^{(1)} = \delta^{(1)} = \gamma^{(1)} = 0. \tag{15}$$

Since the symmetry-axis plane $[x_1, x_3]$ of HTI media is equivalent to the orthorhombic $[x_1, x_3]$ symmetry plane, the definitions of the anisotropic coefficients $\epsilon^{(2)}$, $\delta^{(2)}$, and $\gamma^{(2)}$ [equations (3)–(5)] remain valid for horizontal transverse isotropy. Tsvankin (1997a) and Rüger (1997), who introduced Thomsen-style parameterization for HTI media, called these parameters $\epsilon^{(V)}$, $\delta^{(V)}$, and $\gamma^{(V)}$, respectively:

$$\epsilon^{(V)} \equiv \epsilon^{(2)}, \tag{16}$$

$$\delta^{(V)} \equiv \delta^{(2)}, \tag{17}$$

$$\gamma^{(V)} \equiv \gamma^{(2)}. \tag{18}$$

The coefficient $\delta^{(3)}$ [equation (9)] for HTI media becomes a function of $\epsilon^{(V)}$, $\delta^{(V)}$, and the ratio of the vertical velocities (Tsvankin, 1997a):

$$\delta^{(3)} = \frac{\delta^{(V)} - 2\epsilon^{(V)}\left(1 + \epsilon^{(V)}/f\right)}{\left(1 + 2\epsilon^{(V)}/f\right)\left(1 + 2\epsilon^{(V)}\right)}, \tag{19}$$

where

$$f \equiv 1 - V_{S0}^2/V_{P0}^2. \tag{20}$$

Thus, properties of an HTI medium are determined by a total of five independent parameters: V_{P0}, V_{S0}, $\epsilon^{(V)}$, $\delta^{(V)}$, and $\gamma^{(V)}$. Kinematic signatures of P-waves can be described with sufficient accuracy by the vertical velocity V_{P0}, $\epsilon^{(V)}$, and $\delta^{(V)}$ (Tsvankin, 1997a); these three parameters are supposed to control P-wave NMO velocity as well. Indeed, the NMO velocities from a horizontal reflector in the symmetry planes [equation (11)] in HTI media take the form

$$V_{\rm nmo}^{(1)} = V_{P0}, \tag{21}$$

$$V_{\rm nmo}^{(2)} = V_{P0}\sqrt{1 + 2\,\delta^{(V)}}. \tag{22}$$

The number of independent η coefficients for horizontal transverse isotropy reduces from three to one; in accordance with the definitions of $\eta^{(1,2,3)}$ [equations (12)–(14)], in HTI media with the symmetry axis in the x_1 direction,

$$\eta^{(1)} = 0, \tag{23}$$

$$\eta^{(2)} = \eta^{(V)} = \frac{\epsilon^{(V)} - \delta^{(V)}}{1 + 2\delta^{(V)}}, \tag{24}$$

$$\eta^{(3)} = \frac{\epsilon^{(V)} - \delta^{(V)}}{1 + 2\left(\delta^{(V)} + \epsilon^{(V)}\dfrac{1 - f}{f}\right)} \approx \eta^{(V)}. \tag{25}$$

Although the shear-wave vertical velocity does enter equation (25) through the quantity f, its influence is limited to terms quadratic in the anisotropic parameters and can be ignored (Tsvankin, 1997a). Note that if the symmetry axis points in the x_2-direction, then the parameter $\eta^{(2)} = 0$, while $\eta^{(1)}$ and $\eta^{(3)}$ become identical and equal to $\eta^{(V)}$. Therefore, instead of five P-wave moveout parameters in orthorhombic media, we have only three (V_{P0}, $\epsilon^{(V)}$ or $\eta^{(V)}$, and $\delta^{(V)}$) in an HTI model with a given orientation of the symmetry axis.

NMO ELLIPSES IN A HOMOGENEOUS HTI LAYER

Grechka and Tsvankin (1998) obtained a general equation for azimuthally-varying NMO velocity of any pure mode in the form

$$V_{\rm nmo}^{-2}(\alpha) = W_{11}\cos^2\alpha + 2\,W_{12}\sin\alpha\cos\alpha + W_{22}\sin^2\alpha, \tag{26}$$

where α is the azimuth of the common-midpoint (CMP) line with respect to the x_1-axis, and $\mathbf{W}$ is a symmetric matrix given by

$$W_{ij} = \tau_0\frac{\partial p_i}{\partial x_j}, \qquad (i, j = 1, 2). \tag{27}$$

Here, τ_0 is the one-way zero-offset traveltime, and p_1 and p_2 are the horizontal components of the slowness vector for rays emanating from the zero-offset reflection point; the spatial derivatives of p_i are evaluated at the CMP location. Equation (26) is valid for any inhomogeneous anisotropic medium in which reflection traveltime can be expanded in a Taylor series near the common midpoint. Unless reflection traveltime decreases with offset in a certain direction, the azimuthally-dependent NMO velocity (26) is represented by an ellipse in the horizontal plane. A more detailed discussion of the NMO ellipse can be found in Grechka and Tsvankin (1998) and Tsvankin et al. (1997).

Horizontal reflector

Suppose the symmetry axis of a horizontal HTI layer makes the angle β with the coordinate axis x_1. Adapting the exact expression for normal-moveout velocity [Tsvankin, 1997a, equation (21)], we can represent the P-wave NMO ellipse as

$$V_{\rm nmo}^{-2}(\alpha) = \frac{\cos^2(\alpha - \beta)}{V_{P,\rm nmo}^2} + \frac{\sin^2(\alpha - \beta)}{V_{P0}^2}, \tag{28}$$

where $V_{P,\rm nmo} \equiv V_{\rm nmo}^{(2)} = V_{P0}\sqrt{1 + 2\delta^{(V)}}$ is the NMO velocity in the symmetry-axis direction given by equation (22). Equation (28) can also be obtained from the more general NMO equation in an orthorhombic layer (Grechka and Tsvankin, 1998) by setting the δ coefficient in the isotropy plane to zero.

The semiaxes of the ellipse (28) are aligned with the vertical symmetry planes of the HTI layer, and the NMO velocity is determined by three quantities: the azimuth β of the symmetry axis, the vertical velocity V_{P0}, and the anisotropic coefficient $\delta^{(V)}$. A minimum of three well-separated azimuthal moveout measurements is needed to reconstruct the NMO ellipse and find β, V_{P0}, and $\delta^{(V)}$. Then we can use the vertical velocity to obtain the layer thickness

$$z = V_{P0}\tau_0, \tag{29}$$

where τ_0 is the one-way vertical traveltime.

The accuracy and stability of this inversion procedure and the optimal number and spread of CMP lines are discussed in detail by Al-Dajani and Alkhalifah (1997). Note that unambiguous recovery of V_{P0} and $\delta^{(V)}$ is impossible without identification of the symmetry-axis and isotropy planes, which cannot be done using moveout data alone (in general, it is necessary to include S-wave polarizations or P-wave AVO information). However, the parameter $\delta^{(V)}$ is predominantly negative for fractured formations (Tsvankin, 1997a), and the smaller (semiminor) axis of the NMO ellipse should correspond to the azimuth of the symmetry axis.

Dipping reflector

Tsvankin (1997a) discussed one special case of dip-moveout inversion in HTI media. If the dip plane of the reflector coincides with the symmetry-axis plane, the moveout problem on the dip line becomes two-dimensional because reflected rays do not deviate from the incidence plane. Due to the kinematic equivalence between the symmetry-axis plane of HTI media and any vertical plane in VTI media, the dip-moveout inversion method of Alkhalifah and Tsvankin (1995) is fully applicable to the estimation of $\eta^{(V)}$ on the dip line.

In this paper, we extend this result to a dipping reflector with arbitrary orientation. If the reflector strike is not aligned with either of the symmetry-plane azimuths, the NMO ellipse cannot be represented in the simple form (28) since its semiaxes deviate from the symmetry planes. For instance, for a reflector with the dip plane making an angle of 45° with the symmetry axis in Figure 3, the azimuth of the semimajor axis of the NMO ellipse is equal to 55.6°.

The NMO ellipse from Figure 3 was calculated using an exact equation of Tsvankin et al. (1997) who expressed the components of the matrix **W** [equation (27)] through the slowness vector of the zero offset ray. This equation, valid for any pure mode in a homogeneous layer and arbitrary orientation of the CMP line, has the following form:

$$V_{\rm nmo}^{-2}(\alpha,\, p_1,\, p_2) = \frac{p_1 q_{,1} + p_2 q_{,2} - q}{q_{,11} q_{,22} - q_{,12}^2} \times \left[q_{,22}\cos^2\alpha - 2q_{,12}\sin\alpha\cos\alpha + q_{,11}\sin^2\alpha\right], \quad (30)$$

where $q \equiv q(p_1, p_2) \equiv p_3$ is the vertical component of the slowness vector; $q_{,i}$ and $q_{,ij}$, $(i, j = 1, 2)$ denote the partial derivatives $q_{,i} \equiv \partial q/\partial p_i$ and $q_{,ij} \equiv \partial^2 q/\partial p_i \partial p_j$ that should be evaluated for the zero-offset ray.

The horizontal slownesses (p_1, p_2) of the zero-offset ray can be found using the reflection slopes on zero-offset sections recorded in two different azimuthal directions. Then the vertical slowness q can be determined from the Christoffel equation for a given anisotropic model. Alternatively, if the dip and azimuth of the reflector are known, the Christoffel equation can be solved for the slowness direction orthogonal to the reflector (it corresponds to the zero-offset ray) yielding the slowness components p_1, p_2, and q. The simplest way to obtain the derivatives $q_{,i}$ and $q_{,ij}$ is by implicit differentiation of the Christoffel equation represented through the slowness components (Tsvankin et al., 1997).

Equation (30) can be used to obtain the parameter $\eta^{(V)}$ from the azimuthally-dependent NMO velocity of an arbitrary dipping event. To gain analytic insight into this inversion procedure, we use the weak anisotropy approximation (linearization in the anisotropic coefficients) for the P-wave NMO ellipse in orthorhombic media derived by Grechka and Tsvankin (1999) from equation (30). After substituting the HTI relationships (21)–(25) into Grechka and Tsvankin's equations (A-1)–(A-10), we find

$$V_{\rm nmo}^{-2}(\alpha,\, p_1,\, p_2) = \cos^2\alpha\left\{\frac{1}{V_{P,\rm nmo}^2} - p_1^2 - 2p_1^2\eta^{(V)}\, d_1\right\} - 2\sin\alpha\cos\alpha\, p_1 p_2\left\{1 - 8\eta^{(V)} p_1^2 V_{P0}^2\, d_2\right\} + \sin^2\alpha\left\{\frac{1}{V_{P0}^2} - p_2^2 + 2\eta^{(V)} p_1^4 V_{P0}^2\, d_3\right\}, \quad (31)$$

where

$$d_1 = 6 - 9p_1^2 V_{P0}^2 + 4p_1^4 V_{P0}^4,$$
$$d_2 = 1 - p_1^2 V_{P0}^2,$$
$$d_3 = 1 - 4p_2^2 V_{P0}^2;$$

α is the angle between the CMP line and the symmetry axis.

Since the slowness vector of the zero-offset ray is orthogonal to the reflector, the azimuth of the dip plane depends on the ratio p_2/p_1. Suppose that the the dip plane coincides with the symmetry-axis plane of an HTI layer (i.e., reflector strike is parallel to the axis x_2). Then the zero-offset ray is confined to the $[x_1, x_3]$ plane ($p_2 = 0$), and approximation (31) yields

$$V_{\rm nmo}^{-2}(\alpha,\, p_1,\, p_2) = \cos^2\alpha\left\{\frac{1}{V_{P,\rm nmo}^2} - p_1^2 - 2p_1^2\eta^{(V)}\, d_1\right\} + \sin^2\alpha\left\{\frac{1}{V_{P0}^2} + 2\eta^{(V)} p_1^4 V_{P0}^2\right\}. \quad (32)$$

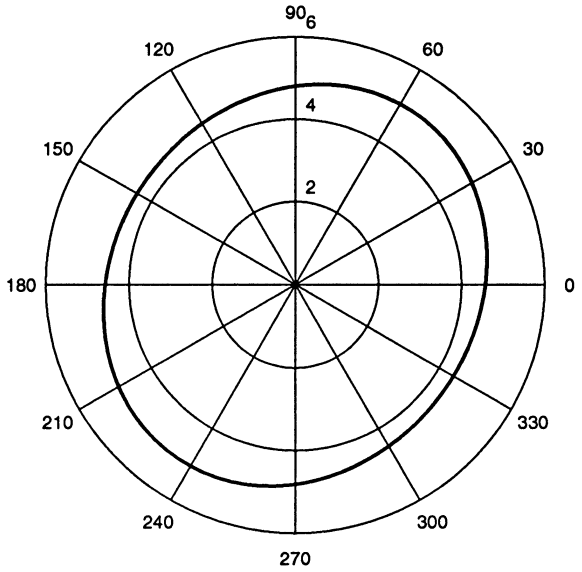

FIG. 3. The P-wave NMO ellipse in an HTI layer above a dipping reflector. The reflector dip is equal to 30°, the azimuth of the dip plane is 45°. The medium parameters correspond to a system of fluid-filled cracks embedded in an isotropic matrix (Rüger and Tsvankin, 1997): $V_{P0} = 4.498$ km/s, $V_{S0} = 2.34$ km/s, $\epsilon^{(V)} = -0.003$, $\delta^{(V)} = -0.088$. The azimuth of the symmetry axis $\beta = 0°$.

The dip-line NMO velocity ($\alpha = 0$) in this case is identical to the corresponding VTI approximation given in Alkhalifah and Tsvankin (1995) and discussed for HTI media by Tsvankin (1997a). Provided the zero-dip NMO velocity in the symmetry-axis plane has been obtained from horizontal events, $V_{\rm nmo}(\alpha = 0, p_1)$ for a dipping event (i.e., $p_1 \neq 0$) is sufficient to determine $\eta^{(\rm V)}$. Equation (32) also shows that the strike-line NMO velocity ($\alpha = 90^\circ$) from a dipping reflector provides a useful redundancy in estimating $\eta^{(\rm V)}$.

If the dip plane of the reflector coincides with the isotropy plane and reflector strike is parallel to the axis x_1 ($p_1 = 0$),

$$V_{\rm nmo}^{-2}(\alpha, p_1, p_2) = \frac{\cos^2\alpha}{V_{P,\rm nmo}^2} + \sin^2\alpha\left\{\frac{1}{V_{P0}^2} - p_2^2\right\}. \quad (33)$$

Clearly, $\eta^{(\rm V)}$ has no influence on both semiaxes of the ellipse (33) and, therefore, cannot be found from moveout data. Therefore, we expect the inversion for $\eta^{(\rm V)}$ to be unstable if the reflector azimuth (i.e., the azimuth of the dip plane) is close to the isotropy plane of the HTI model.

Another situation when $\eta^{(\rm V)}$ is not well constrained by dip moveout is when the reflector is close to horizontal and both slowness components p_1 and p_2 in equation (31) are small. Relevant quantitative estimates can be found in Alkhalifah and Tsvankin (1995) for VTI media and in Grechka and Tsvankin (1999) for orthorhombic media.

PARAMETER ESTIMATION IN AN HTI LAYER

P-wave normal-moveout velocity in HTI media, expressed by equation (30), depends on the symmetry-axis orientation β, the vertical velocity V_{P0}, and the anisotropic coefficients $\epsilon^{(\rm V)}$ (or $\eta^{(\rm V)}$) and $\delta^{(\rm V)}$. Since a single NMO ellipse is determined by three parameter combinations, we need at least two NMO ellipses from reflectors of different dips and/or azimuths to carry out the inversion procedure (i.e., two reflection events provide six equations for four unknowns). Note that in orthorhombic media there are two more unknowns for the same number of equations (Grechka and Tsvankin, 1999), so the inversion procedure in HTI media is expected to be more stable compared to that for orthorhombic models.

Inversion algorithm

In subsequent analysis, we assume that one of the reflectors is horizontal. Then the axis orientation β, V_{P0}, and $\delta^{(\rm V)}$ can be found using the horizontal event, which leaves $\eta^{(\rm V)}$ or $\epsilon^{(\rm V)}$ as the only unknown to be obtained from the NMO ellipse for a dipping reflector. As mentioned above, the negative value of $\delta^{(\rm V)}$ (for fracture-induced HTI media) allows us to distinguish between the azimuths of the symmetry-axis and isotropy planes: the semiminor axis of the NMO ellipse from a horizontal reflector defines the direction of the symmetry axis (normal to the fractures). It may happen that $\delta^{(\rm V)} = 0$, and the NMO ellipse of horizontal events degenerates into a circle. In this case, the azimuth β of the symmetry axis has to be retrieved, along with $\eta^{(\rm V)}$, from the NMO velocity of a dipping event (then, there are three equations for two unknowns).

Our inversion algorithm uses the components of the matrix $\mathbf{W}$ for a dipping event as input data. Assuming that β, V_{P0}, and $\delta^{(\rm V)}$ have already been found, we search for the value of $\eta^{(\rm V)}$ that minimizes the norm of the difference between the measured and theoretical (computed) matrices $\mathbf{W}$:

$$\mathcal{F}\left(\eta^{(\rm V)}\right) = \|\mathbf{W}_{\rm meas} - \mathbf{W}_{\rm theor}\| = \min, \quad (34)$$

where the matrix $\mathbf{W}_{\rm theor}$ is obtained from the exact equation of the NMO ellipse (30). Since $\mathbf{W}_{\rm theor}$ depends on β, V_{P0}, $\delta^{(\rm V)}$, and a single unknown $\eta^{(\rm V)}$, the minimization is carried out by the Golden Section method (Press et al., 1987).

Stability of the estimation of $\eta^{(\rm V)}$

Before discussing the inversion results, we verify whether the shear-wave vertical velocity V_{S0} can be ignored in the parameter-estimation procedure. In agreement with Tsvankin (1997a), although V_{S0} [or the quantity f from equation (20)] does enter the exact phase-velocity equations for the P-wave, its influence on the NMO velocity and inversion results is negligibly small (Figure 4). Therefore, in the examples below we use a "reasonable" value of the V_{S0}/V_{P0} ratio that does not necessarily correspond to the true shear-wave vertical velocity in the model. The parameters of the model used in Figure 4 (including $\epsilon^{(\rm V)} = 0$) are typical for HTI media due to thin fluid-filled cracks in a nonporous matrix (Rüger and Tsvankin, 1997).

If the inversion is performed on error-free data (as in Figure 4), the value of $\eta^{(\rm V)}$ is found with excellent accuracy. The main purpose of the numerical test in Figure 5 is to evaluate the stability of the $\eta^{(\rm V)}$-estimation procedure in the presence of errors in the symmetry-plane NMO velocities from a horizontal reflector. The input data include the exact NMO ellipse for a dipping event (matrix $\mathbf{W}_{\rm meas}$) and the NMO ellipse for a horizontal event that has the correct orientation but a range of errors in the values of the semiaxes (i.e., V_{P0} and $\delta^{(\rm V)}$ are inaccurate but β is exact). For each dipping reflector, we present two sets of the inversion results, one of which is computed for the

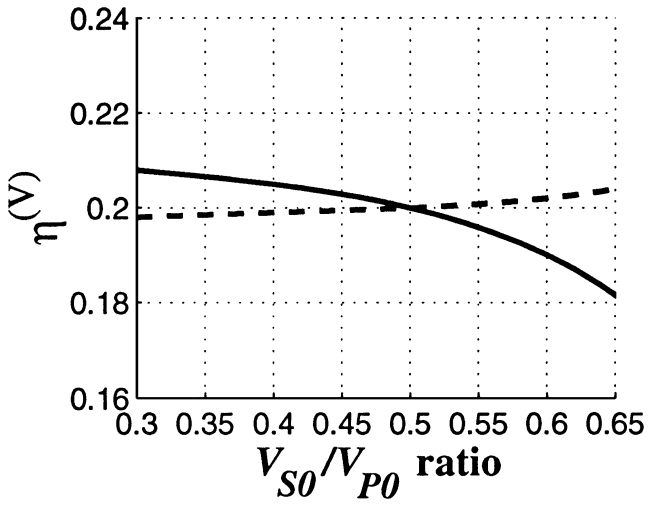

FIG. 4. The influence of the shear-wave vertical velocity V_{S0} on the inversion of the NMO ellipse of a dipping event for $\eta^{(\rm V)}$. The azimuth of the dip plane of the reflector with respect to the symmetry axis is 45°, the dips are 35° (solid line) and 70° (dashed line). The medium parameters are $V_{P0} = 4.0$ km/s, $\epsilon^{(\rm V)} = 0$, $\delta^{(\rm V)} = -0.143$ ($\eta^{(\rm V)} = 0.2$). The actual V_{S0}/V_{P0} ratio is shown on the plot; the inversion was always performed with $V_{S0}/V_{P0} = 0.5$ and actual values of V_{P0}, $\delta^{(\rm V)}$, and β.

HTI model, while the other is obtained under the assumption that the model is orthorhombic (see below).

Assuming the medium to be HTI from the outset of the inversion procedure, we recover $\eta^{(V)}$ (thin solid line) in a stable fashion for the reflectors with dip-plane azimuths of 20° and 45° with respect to the symmetry axis (Figure 5a–d). In accordance with the weak-anisotropy approximation discussed above, the inversion for $\eta^{(V)}$ becomes less stable as the reflector azimuth approaches the isotropy plane (Figure 5e, f). The value of $\eta^{(V)}$ in this case is especially sensitive to errors in the zero-dip NMO velocity in the symmetry-axis plane (Figure 5f). A small deviation of $\eta^{(V)}$ from the actual value even in the absence of errors is caused by the wrong value of the shear-wave vertical velocity intentionally used in the inversion.

HTI versus orthorhombic symmetry in moveout inversion

Since in field experiments we may not know the medium symmetry in advance, it is interesting to carry out the inversion of the NMO ellipse (computed for the actual HTI model) using the algorithm of Grechka and Tsvankin (1999) for the more general orthorhombic medium. In this case, we have to invert three components of the matrix $\mathbf{W}$ for three unknown parameters: $\eta^{(1)}$, $\eta^{(2)}$, and $\eta^{(3)}$. An accurate inversion procedure should yield the expressions for $\eta^{(1,2,3)}$ valid in HTI media: $\eta^{(2)} = \eta^{(V)}$ and $\eta^{(1)} = 0$. Also, for the model from Figure 5, $\epsilon^{(V)} = 0$ and, following from equation (25), $\eta^{(3)} = \eta^{(V)}$ (in general, the last relationship is approximate).

If the zero-dip NMO velocities are exact, we indeed obtain the values that almost satisfy these HTI constraints. The errors in input data, however, get "distributed" among the three η parameters, and it may not be easy to recognize the HTI model by examining the inversion results. For instance, if the reflector azimuth is equal to 20° (Figure 5a, b), the value of $\eta^{(2)}$ stays close to $\eta^{(V)}$, but $\eta^{(1)}$ and $\eta^{(3)}$ show substantial variations under the influence of errors in V_{P0}. This result is in agreement with the conclusion of Grechka and Tsvankin (1999) that if the dip plane of the reflector is near the $[x_1, x_3]$ symmetry plane, NMO

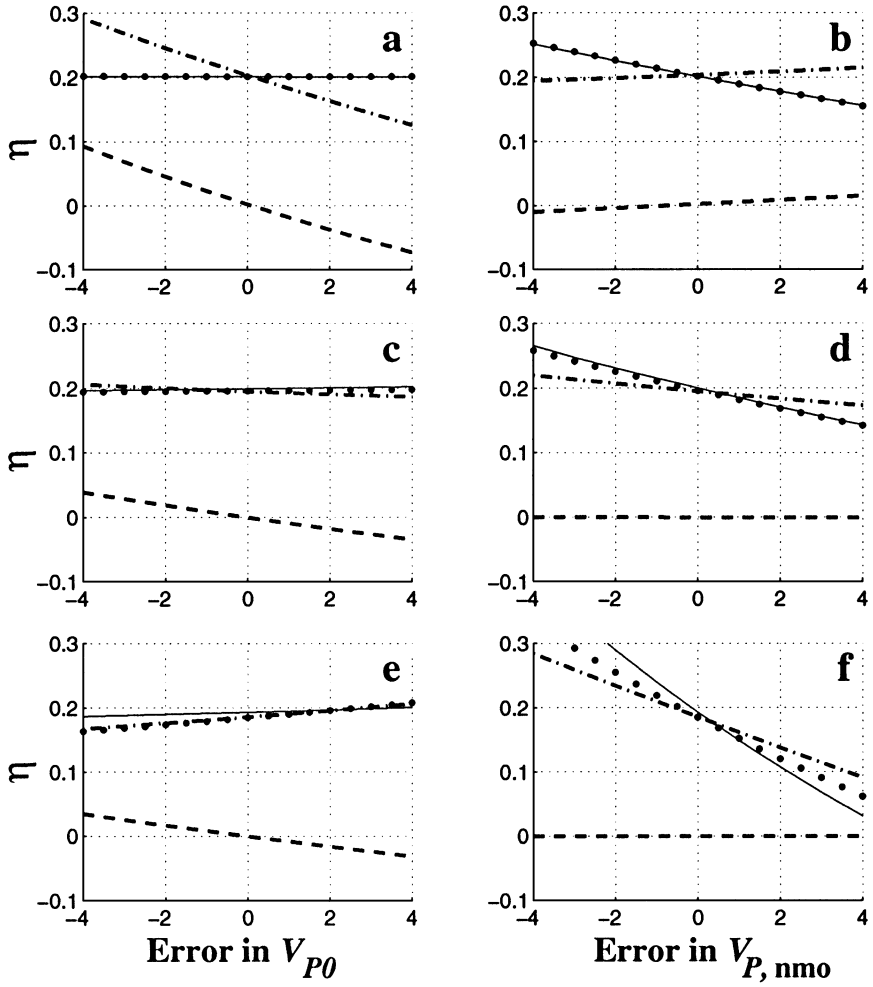

FIG. 5. Inversion of the NMO ellipse for a dipping event in the presence of errors in the symmetry-plane NMO velocities from a horizontal reflector (in percent). The reflector dip is 50°; the azimuth of the dip plane is different for each row: 20° (a, b), 45° (c, d), and 70° (e, f). The layer parameters are $V_{P0} = 4.0$ km/s, $\epsilon^{(V)} = 0$, $\delta^{(V)} = -0.143$ ($\eta^{(V)} = 0.2$). The thin solid line denotes $\eta^{(V)}$ obtained by assuming the HTI model in the inversion procedure. Under the assumption that the model is orthorhombic, we computed $\eta^{(1)}$ (dashed line), $\eta^{(2)}$ (dotted line), and $\eta^{(3)}$ (dash-dotted line). For the HTI model used to generate the data, $\eta^{(2)} = \eta^{(3)} = \eta^{(V)} = 0.2$ and $\eta^{(1)} = 0$.

velocity constrains the difference between $\eta^{(1)}$ and $\eta^{(3)}$, but not the individual values of the coefficients. The HTI signature is most apparent in the inverted values for a reflector azimuth of 45° (Figure 5c, d), where $\eta^{(1)} \approx 0$ and $\eta^{(2)} \approx \eta^{(3)} \approx 0.2$ for the whole range of errors in the zero-dip NMO velocities. Thus, to recognize the HTI symmetry in the inversion results for orthorhombic media in a reliable fashion, the dip plane of the reflector should make an angle of 30–50° with the symmetry axis.

A more direct way to identify the symmetry system is by checking whether the inverted HTI model provides a satisfactory fit to the NMO ellipses. For instance, in Figure 5b, the NMO ellipse of the dipping event for the obtained HTI model does not deviate from the exact ellipse by more than 1%. In such a case, performing inversion for the more complicated orthorhombic model is hardly justified because it would only lead to overfitting the data.

If the medium has the orthorhombic symmetry and is sufficiently different from HTI [i.e., equations (23)–(25) are not satisfied with acceptable accuracy], the best-fit HTI model found from moveout inversion cannot adequately explain the observed moveout velocities. As illustrated by the example in Figure 6, the HTI algorithm applied to orthorhombic data succeeds in fitting the NMO ellipse for a horizontal event by distorting the vertical velocity V_{P0} and making corresponding adjustments in the parameter $\delta^{(V)}$. However, as discussed above, the remaining parameter $\eta^{(V)}$ has to be found from three nonlinear equations describing the NMO ellipse for a dipping event. Since the data are generated for orthorhombic media and do not comply with the HTI relationships, these equations cannot be accurately solved for any value of $\eta^{(V)}$. As a result, the best-fit HTI model fails to match the NMO ellipse for the dipping event (Figure 6). We conclude that if the medium has orthorhombic or lower symmetry, the HTI model is unable to fit P-wave moveout data provided NMO ellipses for a horizontal and a dipping reflection events are available.

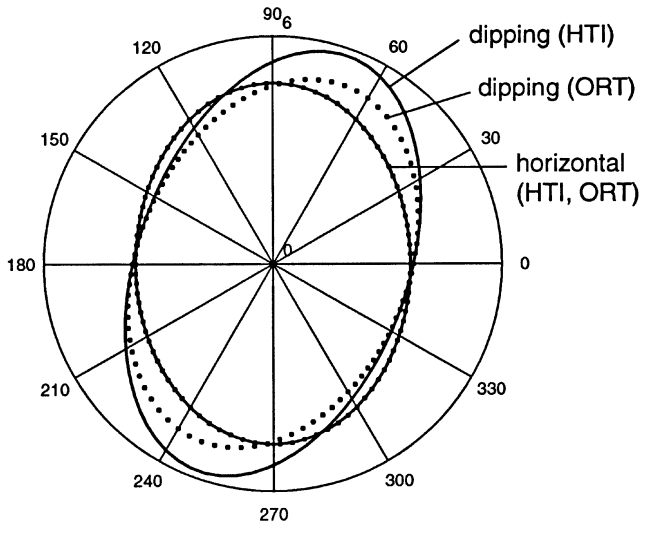

FIG. 6. HTI inversion of the NMO ellipses computed for an orthorhombic model with $V_{P0} = 4.388$ km/s, $\epsilon^{(1)} = -0.2$, $\epsilon^{(2)} = -0.15$, $\delta^{(1)} = 0.1$, $\delta^{(2)} = -0.155$, and $\delta^{(3)} = 0.101$ ($\eta^{(1)} = 0.008$, $\eta^{(2)} = -0.25$, $\eta^{(3)} = -0.16$). Dotted lines—input NMO ellipses from a horizontal interface and a dipping reflector (the dip-plane azimuth is 40°, dip = 45°). Solid lines—the ellipses for the best-fit HTI model obtained from the inversion; the model parameters are $V_{P0} = 4.752$ km/s, $\epsilon^{(V)} = -0.272$, $\delta^{(V)} = -0.213$ ($\eta^{(V)} = -0.103$).

MOVEOUT INVERSION IN VERTICALLY INHOMOGENEOUS HTI MEDIA

The inversion approach described above can be extended to horizontally layered HTI media above a dipping reflector using the generalized Dix equation (Tsvankin et al., 1997). This equation expresses the exact effective NMO velocity through the average of the matrices $\mathbf{W}$ responsible for the interval NMO ellipses [equations (26) and (27)]:

$$\mathbf{W}^{-1}(L) = \frac{1}{\tau(L)} \sum_{\ell=1}^{L} \tau_\ell \, \mathbf{W}_\ell^{-1}, \tag{35}$$

where $\mathbf{W}(L)$ and $\mathbf{W}_\ell$ define the effective and interval NMO ellipses, respectively, τ_ℓ are the interval zero-offset traveltimes, and $\tau(L) = \sum_{\ell=1}^{L} \tau_\ell$. Equation (35) is valid for reflections from a dipping interface beneath an arbitrary anisotropic vertically inhomogeneous overburden.

Rewriting equation (35) in the differentiation form yields

$$\mathbf{W}_\ell^{-1} = \frac{\tau(\ell)\mathbf{W}^{-1}(\ell) - \tau(\ell-1)\mathbf{W}^{-1}(\ell-1)}{\tau(\ell) - \tau(\ell-1)}. \tag{36}$$

It should be emphasized that the interval matrices $\mathbf{W}_\ell$ in all layers are evaluated for the horizontal slownesses p_1 and p_2 of the zero-offset ray. Even if the medium contains a throughgoing interface with constant dip (e.g., a fault plane), zero-offset reflections from this interface in different layers will not generally have the same values of p_1 and p_2. As a result, equation (36) should be applied through a stripping procedure that involves layer-by-layer determination of the moveout parameters starting from the subsurface layer and continuing downward (Grechka and Tsvankin, 1999).

Figure 7 illustrates the difference between the (exact) averaging of NMO ellipses and conventionally used (approximate) rms averaging of NMO velocities at a certain azimuth. The effective NMO ellipse from the bottom of the two-layer HTI model (dashed line) was computed by applying equation (35) to the interval NMO ellipses. Note that at azimuth 69°, where two effective ellipses (solid and dashed) intersect and the effective NMO velocities are equal to each other, the interval NMO velocity in the second layer (dotted) is smaller than both effective ones. This interval velocity would be overestimated by the conventional Dix differentiation of the NMO velocities at this azimuth that would just yield the effective value. Likewise, the interval NMO ellipses (solid and dotted) intersect at an azimuth of 61°, where the effective NMO ellipse computed from equation (35) (dashed) yields a greater effective NMO velocity than both interval values. In such a case, conventional Dix averaging underestimates the effective NMO velocity. A more detailed comparison of the exact NMO equation (35) and the rms averaging of NMO velocities is given in Tsvankin et al. (1997).

SYNTHETIC EXAMPLE

To evaluate the performance of our parameter-estimation methodology, we applied it to the inversion of ray-traced

traveltimes in a stratified HTI model with a dipping reflector cutting through all layers (Table 1). We computed the exact P-wave reflection traveltimes from horizontal and dipping reflectors along 6 azimuths with an increment of 30°. Large offsets were muted out to maintain a spreadlength-to-depth ratio of 1 for all reflections. Using the conventional hyperbolic approximation for reflection moveout, we calculated the best-fit moveout velocities at each azimuth and reconstructed the corresponding NMO ellipses. After carrying out the moveout inversion in the first layer, we used the generalized Dix equation (36) to recover the interval NMO ellipses for the horizontal and dipping events in the second layer and obtain the layer parameters. Then we repeated this operation for the last (third) layer; a more detailed description of this layer-stripping procedure is given in Grechka and Tsvankin (1999).

The maximum error in the interval vertical velocity V_{P0} and the layer thicknesses z is just 0.6% (see Table 1), whereas the errors in the interval anisotropic coefficients $\epsilon^{(V)}$ and $\delta^{(V)}$ are limited by 0.03. The orientation of the symmetry axis, which varied from layer to layer, was accurately restored as well. The small inversion errors are caused by the influence of nonhyperbolic moveout on the moveout velocities, which served as input data for parameter estimation. Our results indicate that P-wave reflection moveout for conventional offsets close to the reflector depth does not deviate much from a hyperbola. The same conclusion was drawn by Grechka and Tsvankin (1999) in their study of reflection moveout in orthorhombic media.

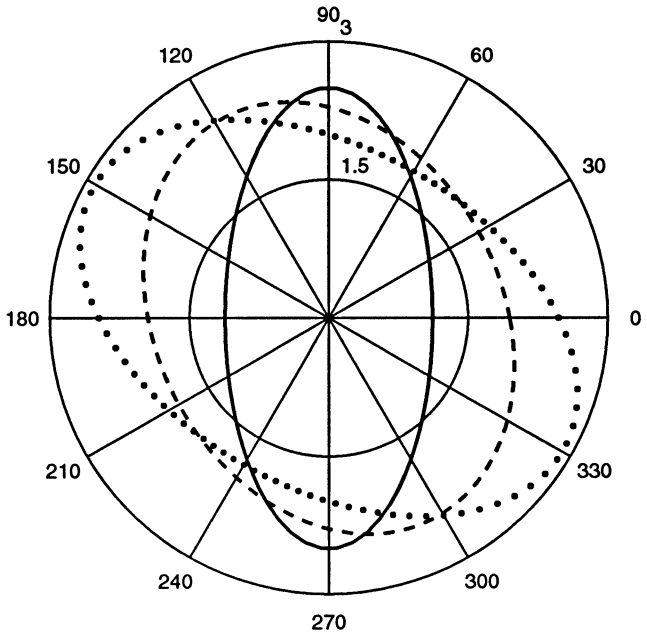

FIG. 7. Azimuthally-dependent NMO velocities in an HTI model that consists of two horizontal layers. Solid line—the NMO ellipse from the bottom of the first layer; dotted line—the interval ellipse for the second layer; dashed line—the effective ellipse from the bottom of the second layer. The relevant parameters of the first layer are $V_{P0,1} = 2.5$ km/s, $\delta_1^{(V)} = -0.4$, $\beta_1 = 0°$, z_1 (thickness) =1.0 km; for the second layer, $V_{P0,2} = 2.9$ km/s, $\delta_2^{(V)} = -0.3$, $\beta_2 = 60°$, $z_2 = 1.0$ km.

PHYSICAL PROPERTIES OF CRACKS FROM MOVEOUT INVERSION

The azimuthal variation of P-wave NMO velocity can be used to determine the direction of the symmetry axis and, therefore, identify the fracture orientation. Also, the results of moveout inversion for HTI media can be directly related to the physical properties of crack systems important in characterization of fractured reservoirs. One of these properties is the crack density (the product of the number of cracks per unit volume and their mean cubed diameter), which is proportional to the shear-wave splitting parameter $\gamma^{(S)}$ at vertical incidence (Thomsen, 1995). Although P-wave moveout inversion cannot yield the shear-wave splitting parameter directly, $\gamma^{(S)}$ [equation (10)] can be calculated from $\epsilon^{(V)}$ and $\delta^{(V)}$ using the constraint on the stiffness coefficients for the HTI model due to thin parallel cracks (Tsvankin, 1997a):

$$\gamma^{(S)} = \frac{V_{P0}^2}{2\,V_{S0}^2}\,\frac{\epsilon^{(V)}[2 - 1/f] - \delta^{(V)}}{1 + 2\epsilon^{(V)}/f + \sqrt{1 + 2\delta^{(V)}/f}}; \qquad (37)$$

f was defined in equation (20). Although equation (37) involves the shear-wave vertical velocity that cannot be obtained from P-wave moveout data, a rough estimate of V_{P0}/V_{S0} is sufficient for applying this expression for $\gamma^{(S)}$ in detecting "sweet spots" of high crack density in fractured reservoirs.

Once the set of all three anisotropic coefficients ($\gamma^{(S)}$, $\epsilon^{(V)}$, and $\delta^{(V)}$) has been recovered, it can be used to deduce more information about the properties of the crack system. For instance, for thin fluid-filled cracks in the absence of equant porosity, $\epsilon^{(V)} \approx 0$, while $\gamma^{(S)} \approx -\delta^{(V)}$ (Thomsen, 1995; Tsvankin, 1997a). In contrast, for dry cracks typically $\epsilon^{(V)} \approx \delta^{(V)} < 0$, and $\gamma^{(S)}$ is much smaller than $|\epsilon^{(V)}|$ (Rüger and Tsvankin, 1997).

DISCUSSION AND CONCLUSIONS

Normal-moveout velocity of P waves for horizontal transverse isotropy is controlled by the azimuth of the symmetry axis β (normal to the fractures), the vertical velocity V_{P0}, and the

Table 1. Comparison of the actual and inverted parameters for a three-layer HTI model with a throughgoing dipping reflector (e.g., a fault plane). The reflector dip is 40°, the azimuth of the dip plane is 60°. The spreadlength-to-depth ratio is equal to unity for all events.

	Actual values					Inverted values				
Layer	z (km)	V_{P0} (km/s)	$\epsilon^{(V)}$	$\delta^{(V)}$	β (degrees)	z (km)	V_{P0} (km/s)	$\epsilon^{(V)}$	$\delta^{(V)}$	β (degrees)
1	1.000	2.500	−0.100	−0.200	0.00	0.994	2.485	−0.130	−0.178	0.07
2	0.700	2.900	−0.050	−0.100	20.00	0.701	2.902	−0.040	−0.090	19.23
3	0.300	3.200	−0.200	−0.300	40.00	0.301	3.206	−0.181	−0.289	40.05

anisotropic coefficients $\epsilon^{(V)}$ and $\delta^{(V)}$. For purposes of moveout inversion, $\epsilon^{(V)}$ is convenient to replace with the "anellipticity" coefficient $\eta^{(V)}$ responsible for dip moveout. In this paper, we show that all four parameters can be recovered in a stable fashion using azimuthally-dependent NMO velocities from a horizontal and a dipping reflector. The NMO ellipse for a horizontal event can be inverted for the symmetry-axis orientation β, V_{P0}, and $\delta^{(V)}$, and the remaining coefficient $\eta^{(V)}$ can be obtained from the moveout for a dipping reflector. If $\delta^{(V)} = 0$, the NMO velocity from a horizontal reflector is independent of azimuth, and the angle β should be recovered (along with $\eta^{(V)}$) from the NMO ellipse of a dipping event.

Our inversion technique is based on the exact NMO equation for a homogeneous layer of arbitrary symmetry given by Tsvankin et al. (1997) and follows the methodology developed by Grechka and Tsvankin (1999) for the more general orthorhombic model. In principle, it is possible to carry out the inversion assuming that the model is orthorhombic and identify the HTI symmetry by the specific relationships between the obtained η coefficients. Although such an algorithm works well on error-free data, it can give ambiguous results in field applications because the errors in input information tend to be distributed among the three orthorhombic η parameters in a complicated fashion. A better approach is to assume the HTI symmetry from the outset of the parameter-estimation procedure and verify this assumption by the inversion results. If the inverted HTI model provides a good fit to the data (i.e., to the NMO ellipses of a horizontal and a dipping event), then it is not warranted to move on to a more complicated orthorhombic model. On the other hand, if the inversion algorithm is unable to find a suitable set of the HTI parameters, it is a strong indication that the reservoir has the orthorhombic or lower symmetry (such an example was given above).

Analytic and numerical results show that the parameter $\eta^{(V)}$ can be obtained with good accuracy for a wide range of reflector dips and azimuths, and is especially well-determined if the dip plane of the reflector is close to the direction of the symmetry axis. The only range of reflector azimuths unfavorable for $\eta^{(V)}$ inversion corresponds to a vicinity of the isotropy plane.

We also extended our inversion technique to vertically inhomogeneous HTI media above an arbitrary-oriented dipping reflector using the generalized Dix equation (Tsvankin et al., 1997). As a result of the Dix-type layer-stripping procedure, we find the interval values of β, V_{P0}, $\eta^{(V)}$ ($\epsilon^{(V)}$), $\delta^{(V)}$, and the interval thickness z. Application of the Dix differentiation imposes obvious restrictions on the minimum thickness of the interval, which are well known for isotropic media and remain valid in the presence of anisotropy.

The inversion algorithm was tested on ray-traced traveltime data generated for a stratified HTI model with depth-varying orientation of the symmetry axis. All interval values were restored with excellent accuracy, which indicates that nonhyperbolic moveout does not seriously distort moveout velocity on conventional spreads close to the reflector depth.

An attractive feature of parameter estimation in HTI media is the possibility to find the true vertical velocity and reflector depth from P-wave moveout data. In contrast, surface data acquired over VTI and orthorhombic media do not provide enough information for the transition from moveout to vertical velocities. Therefore, P-wave moveout inversion for horizontal transverse isotropy allows one to build a velocity model for depth processing, as opposed to time processing for VTI and orthorhombic media.

Another advantage of the HTI model is a relatively simple relationship between the moveout parameters and the physical properties of the crack system. The direction of the symmetry axis yields the crack orientation, while the parameters $\epsilon^{(V)}$ [calculated from $\eta^{(V)}$ using equation (24)] and $\delta^{(V)}$ can be combined to estimate the shear-wave splitting coefficient $\gamma^{(S)}$ and the crack density (Tsvankin, 1997a). Furthermore, the relationship between $\epsilon^{(V)}$, $\delta^{(V)}$, and the crack density depends on the contents of the cracks, which makes it possible to discriminate between fluid-filled and dry cracks using P-wave moveout data. Of course, since this method is based on kinematic analysis, the reservoir has to be thick enough to change the reflection traveltimes in a measurable way.

Although P-wave moveout alone can provide us with useful information, it is beneficial to combine it with amplitude-variation-with-offset (AVO) signature or results of shear-wave splitting analysis. For instance, the P-wave AVO gradient in HTI media depends on a combination of $\delta^{(V)}$ and $\gamma^{(S)}$ (Rüger, 1997). Therefore, AVO inversion can be used to evaluate the shear-wave splitting parameter, if $\delta^{(V)}$ has been found from P-wave moveout. If shear data are available, the coefficient $\gamma^{(S)}$ can be obtained directly from the time delay between two split shear waves at near-vertical incidence. Then, it can be combined with the results of P-wave moveout inversion (i.e., with the parameters $\delta^{(V)}$ and $\epsilon^{(V)}$) to study the contents of the cracks. In addition, both the AVO response and shear-wave polarizations yield an independent estimate of the azimuth of the symmetry axis. Of course, the combination of moveout and amplitude analyses makes certain assumptions about the character of the distribution of the elastic parameters (e.g., piecewise constant).

ACKNOWLEDGMENTS

This research was initiated during P. Contreras' visit to the Center for Wave Phenomena, Colorado School of Mines, in 1996. P. Contreras is grateful to PDVSA-INTEVEP for supporting his stay at CSM. The work was partially sponsored by the members of the Consortium Project on Seismic Inverse Methods for Complex Structures at CWP and by the US Department of Energy.

REFERENCES

Al-Dajani, A., and Alkhalifah, T., 1997, Reflection moveout inversion in azimuthally anisotropic media: Accuracy and acquisition requirements: 67th Ann. Internat. Mtg., Soc. Expl. Geophys., Expanded Abstracts, 1230–1233.

Al-Dajani, A., and Tsvankin, I., 1998, Nonhyperbolic reflection moveout for horizontal transverse isotropy: Geophysics, **63**, 1738–1753.

Alkhalifah, T., and Tsvankin, I., 1995, Velocity analysis in transversely isotropic media: Geophysics, **60**, 1550–1566.

Grechka, V., and Tsvankin, I., 1998, 3-D description of normal moveout in anisotropic inhomogeneous media: Geophysics, **63**, 1079–1092.

Grechka, V., and Tsvankin, I., 1999, 3-D moveout velocity analysis and parameters estimation for orthorhombic media: Geophysics, **64**, 820–837.

Press, W. H., Flannery, B. P., Teukolsky, S. A., and Vetterling, W. T., 1987, Numerical recipes: The art of scientific computing: Cambridge Univ. Press.

Rüger, A., 1997, P-wave reflection coefficients for transversely isotropic models with vertical and horizontal axis of symmetry: Geophysics, **62**, 713–722.

Rüger, A., and Tsvankin, I., 1997, Using AVO for fracture detection: Analytic basis and practical solutions: The Leading Edge, **16**, 1429–1434.

Schoenberg, M., and Helbig, K., 1997, Orthorhombic media: Modeling elastic wave behavior in a vertically fractured earth: Geophysics, **62**, 1954–1974.
Thomsen, L., 1986, Weak elastic anisotropy: Geophysics, **51**, 1954–1966.
——— 1988, Reflection seismology over azimuthally anisotropic media: Geophysics, **53**, 304–313.
——— 1995, Elastic anisotropy due to aligned cracks in porous rock: Geophys. Prosp., **43**, 805–830.
Tsvankin, I., 1995, Normal moveout from dipping reflectors in anisotropic media: Geophysics, **60**, 268–284.
——— 1997a, Reflection moveout and parameter estimation for horizontal transverse isotropy: Geophysics, **62**, 614–629.
——— 1997b, Anisotropic parameters and *P*-wave velocity for orthorhombic media: Geophysics, **62**, 1292–1309.
Tsvankin, I., Grechka, V., and Cohen, J. K., 1997, Generalized Dix equation and modeling of normal moveout in inhomogeneous anisotropic media: 67th Ann. Internat. Mtg., Soc. Expl. Geophys., Expanded Abstracts, 1246–1249.
Wild, P., and Crampin, S., 1991, The range of effects of azimuthal isotropy and EDA anisotropy in sedimentary basins: Geophys. J. Internat., **107**, 513–529.